

Palaeomagnetism and $^{40}\text{Ar}/^{39}\text{Ar}$ dating from Lower Jurassic rocks in Gastre, central Patagonia: further data to explore tectonomagmatic events associated with the break-up of Gondwana

CLAUDIA BEATRIZ ZAFFARANA^{1,2} & RUBÉN SOMOZA^{1,2*}

¹*Departamento de Ciencias Geológicas, FCEyN, Universidad de Buenos Aires, Pabellón 2, Ciudad Universitaria, C1428EHA, Buenos Aires, Argentina*

²*IGIBA-CONICET, Argentina*

**Corresponding author (e-mail: somoza@gl.fcen.uba.ar)*

Abstract: New $^{40}\text{Ar}/^{39}\text{Ar}$ data indicate ages of *c.* 185 Ma for the Lonco Trapial volcanic field in Gastre, north-central Patagonia, implying that this andesitic unit is roughly coeval with the Marifil silicic province that crops out in the eastern part of northern Patagonia. These volcanic fields are therefore roughly coeval with the Karoo–Ferrar large igneous province, further contributing to the huge, 185–180 Ma magmatic outpouring in southern Gondwana. The comparison of palaeomagnetic results from the unit with Early Jurassic reference palaeopoles suggests that Gastre records a small, anticlockwise finite rotation with respect to stable South America. This contrasts sharply with the large clockwise rotation recorded by roughly coeval dolerites from the Falkland/Malvinas Islands, and argues against a direct relationship between the rotation of the islands and the tectonic activity in Gastre. The results support previous suggestions that the Gastre Fault System is not the locus of major strike-slip displacement activity in the Jurassic as some workers have suggested. Taken as a whole, palaeomagnetic data from Patagonia suggest a more complex than previously thought pattern of distributed and variable deformation during the early stages of Gondwana breakup. The crustal block boundaries in the region remain cryptic.

Supplementary material: $^{40}\text{Ar}/^{39}\text{Ar}$ analytical procedures and expanded data are available at <http://www.geolsoc.org.uk/SUP18522>.

The Triassic–Jurassic configuration of terranes in Western Gondwana is the subject of some uncertainty with respect to the major cratonic nuclei. Furthermore, the processes that promoted the motion of each of the terranes to their present-day position, as well as the structures that accommodated these motions, are poorly known (e.g. Dalziel & Grunow 1992; Marshall 1994; DiVenere *et al.* 1996; König & Jokat 2006; Martin 2007; Eagles & Vaughan 2009). This collage of early Mesozoic landmasses formed a Pan-Pacific mobile belt outboard of the major cratonic nuclei of Gondwana. In this context Patagonia is a major and enigmatic terrane and is the focus of this study.

A major contribution to the pre-breakup palaeogeography of the region was provided by palaeomagnetic results from *c.* 180 Ma dolerites in West Falkland, which indicate *c.* 100° clockwise rotation possibly during Jurassic times (Taylor & Shaw 1989). This rotation agrees with stratigraphic and structural correlations that point to a pre-breakup position of the island to the east of, and in continuity with the Cape foldbelt (e.g. Adie 1952; Curtis & Hyam 1998). The driving mechanism for the rotation of the whole Falkland/Malvinas platform remains elusive. Nevertheless, whatever the process considered, all previous models invoke a simultaneous westward escape of Patagonia either as a single microplate or as a collection of crustal blocks (e.g. Rapela & Pankhurst 1992; Ben-Avraham *et al.* 1993; Marshall 1994; Barker 1999; Martin 2007) to accommodate the Falkland/Malvinas rotation.

The most popular mechanism considered for the accommodation of the westward motion of Patagonia with respect to stable South America is dextral sliding along the Gastre Fault System (Fig. 1a), which was interpreted as an intercontinental, tens of kilometres wide, dextral strike-slip zone (Rapela & Pankhurst 1992).

However, Rapela *et al.* (2005) recognized that the amount of dextral displacement in the Gastre Fault System invoked in the above models is unrealistic. Moreover, recent work (von Gosen & Loske 2004; Zaffarana *et al.* 2010, 2012) has shown that the geological record in Gastre shows neither the intensity nor the kinematics or indeed the timing of deformation as required in previous Gondwana breakup models. Currently, the transcontinental fault zones required to accommodate the relative motion between the Patagonian blocks remain cryptic and unobserved (Zaffarana *et al.* 2010, 2012).

In this paper we report palaeomagnetic results and $^{40}\text{Ar}/^{39}\text{Ar}$ ages from Jurassic rocks that rest unconformably on the Late Triassic granitoids of the Central Patagonian Batholith (Rapela *et al.* 1992; Zaffarana *et al.* 2010). These Triassic granitoids were considered as the main carrier of the deformational evidence for supporting the transcontinental, dextral kinematics commonly attributed to the Gastre Fault System (e.g. Rapela & Pankhurst 1992). The isotopic data indicate that the sampled lavas were erupted in the Early Jurassic, with ages comparable with those of both the dolerites in the Falkland/Malvinas Islands and the magmatism in the Karoo–Ferrar large igneous province (LIP). The palaeomagnetic results show that Gastre records an anticlockwise finite rotation with respect to stable South America, which argues against a direct relationship between the large clockwise rotation of the Falkland/Malvinas platform and the Jurassic deformation in Gastre.

The Lonco Trapial Formation at Gastre

The Gastre area, located in the central–southern sector of the North Patagonian Massif (Fig. 1), is characterized by widespread outcrops of the Central Patagonian Batholith, which is formed by two

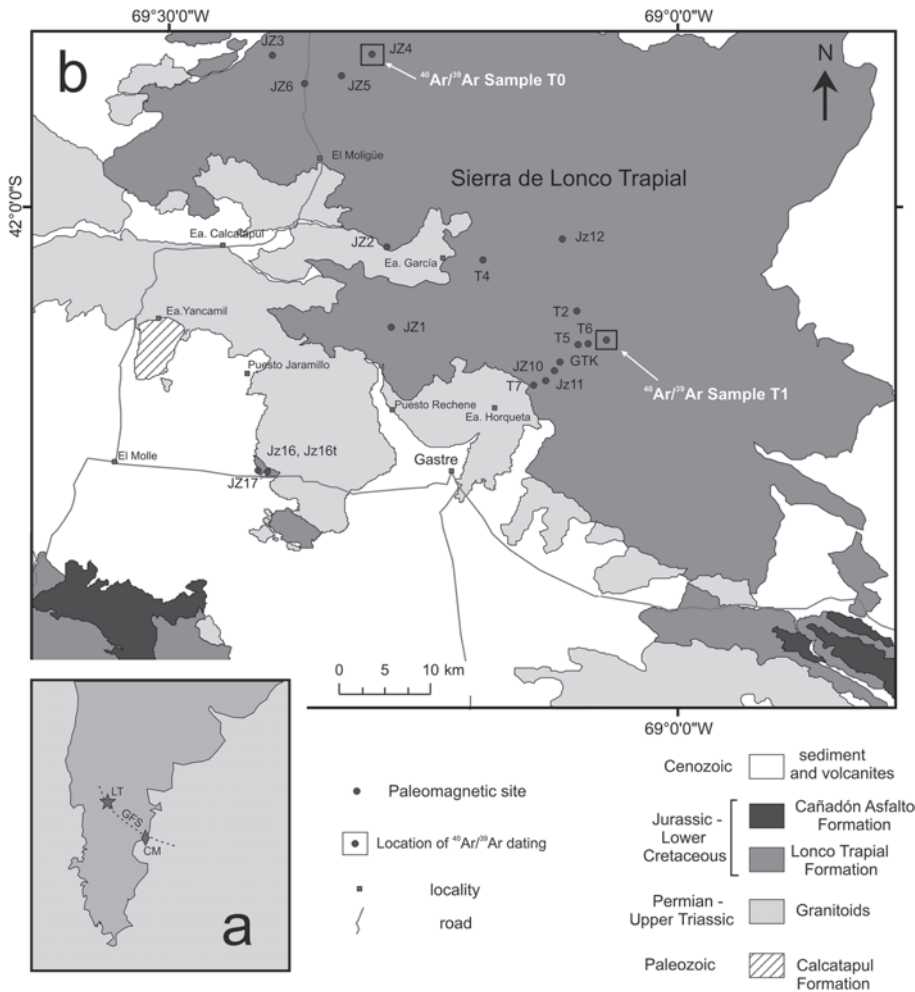


Fig. 1. (a) Proposed trace of the Gastre Fault System (GFS) as suggested by Rapela & Pankhurst (1992). LT and CM denote the location of sampling zones of this study and of the study of Iglesia Llanos *et al.* (2003), respectively. (b) Geological map of the study area showing location of sampling sites.

suites of Late Triassic (*c.* 220–210 Ma) I-type granitoids (Rapela *et al.* 1992; Zaffarana *et al.* 2010). Resting on a highly irregular palaeosurface carved in these granitoids is a Jurassic volcano-sedimentary unit, formerly known as the Taquetren Formation but now included in the Lonco Trapial Formation (e.g. Page & Page 1993), whose type localities crop out further south.

The Lonco Trapial Formation at Gastre is composed of a volumetrically important andesitic eruptive suite associated with thick conglomerates and locally important tuffaceous layers and minor andesitic dykes. The volcanic facies is mainly represented by andesites, breccias, and subordinate ignimbrites. Sparse outcrops of rhyolitic and andesitic dykes represent associated sub-volcanic facies. The sedimentary facies is represented by thick conglomerates, which in the main sampling zone are almost exclusively composed of volcanic boulders, although blocks of granitoids are common in the conglomerates from the southern outcrops shown in Figure 1b. Subordinate to the conglomerates there are thinner units of pelites and tuffaceous sandstones.

The physical continuity of amalgamated volcanic facies can be traced over distances of tens of kilometres in the volcanic massif forming the Sierra de Lonco Trapial (Fig. 1b). Palaeohorizontal was confidently determined at most sampling sites by diverse observations such as intercalated sedimentary layers, *c.* 0.5 km scale triangulation of the topographic level from single conglomerate–lava contacts, measurements of the disposition of *in situ* metre-scale fossil tree trunks in tuffaceous sandstones, observation of

contacts of ignimbrite bodies, and measurements of compaction planes provided by fiamme. Overall most sites in the sampled region (Fig. 1b) were found to be subhorizontal in attitude.

Geochronology

The Lonco Trapial Formation has been traditionally assigned to the Middle Jurassic *sensu lato* (e.g. Rapela *et al.* 2005) although an interfingering stratigraphic relationship with supposedly older Jurassic units has been observed in some localities. Recently, Silva Nieto (2005) reported, without providing analytical data, a 173.1 ± 9.4 Ma whole-rock K/Ar age from an andesite cropping out *c.* 150 km SSW of Gastre. In this paper we report three $^{40}\text{Ar}/^{39}\text{Ar}$ step-heating ages on amphibole grains (Fig. 2) from samples from two outcrops in the study area (see location in Fig. 1b). These single grain analyses were carried out on grains of the order of 251 and 178 μm (60–80 mesh grain size). The dated samples are andesitic lavas cropping out at $41^\circ 51' 14.7''\text{S}$, $69^\circ 18' 02''\text{W}$ and $42^\circ 7' 52.11''\text{S}$, $69^\circ 4' 19.55''\text{W}$ (samples T0 and T1 respectively in Fig. 1b).

Sample T0 is an andesitic lava ($\text{SiO}_2 = 62.39\%$; $\text{K}_2\text{O} = 1.98\%$; Franzese *et al.* 2002) with hornblende and plagioclase crystal-clasts (5% of the rock) immersed in a pilotaxitic-looking ground-mass, where long plagioclase microlites in general show good flow-structure. Hornblende crystals are fresh and exhibit green to brown pleochroism and have resorption borders. They can measure

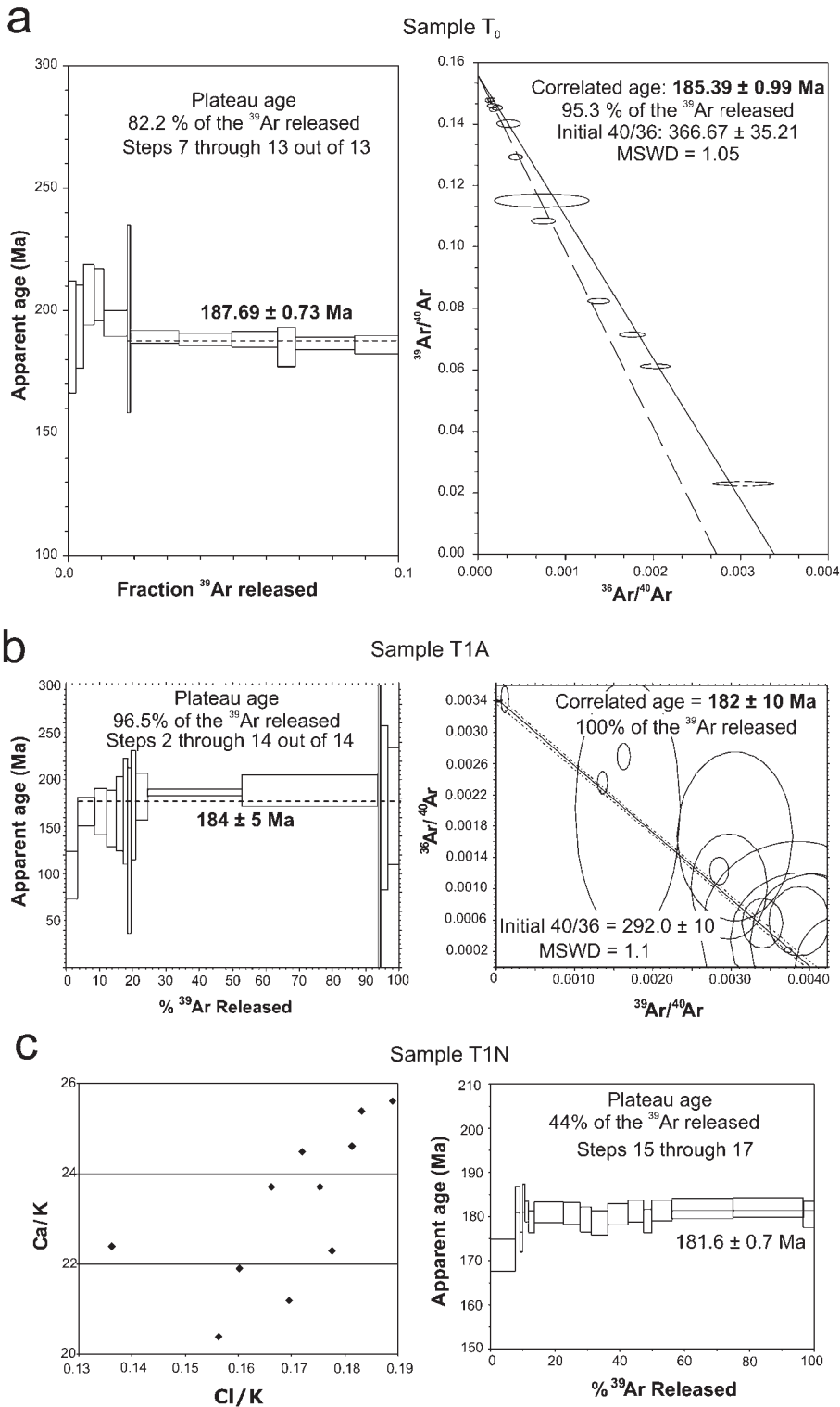


Fig. 2. ⁴⁰Ar/³⁹Ar age spectra and isochrons obtained on single grains of amphibole from andesitic lavas of the Lonco Trapial Formation. Results from samples T0 (a), T1A (b) and T1N (c).

up to 10 mm, but their average size is significantly smaller because they appear frequently broken. Plagioclase crystals may also be fractured, and have polysynthetic twinning, zonality, cribate texture and albitic rims. The groundmass (95% of the rock) is composed of plagioclase, opaque minerals, hornblende and clays.

Sample T1 is an andesitic lava with amphibole and plagioclase phenocrysts in a greyish green pilotaxitic groundmass. Phenocrysts (50% of the rock) are represented by hornblende, plagioclase,

clinopyroxene, opaque minerals and biotite. Plagioclase phenocrysts (60% of phenocrysts) are euhedral and zonal, and have cribate texture. They are intensely altered to sericite and clays. Sometimes they have nuclei of more calcic composition, which show more intense alteration than crystal borders. They can measure up to 30 mm in length. Hornblende phenocrysts are large (c. 10 mm), euhedral and fresh, and represent 10% of the rock. They are slightly pleochroic from green to light green and may

Table 1. Summary of geochronological data (errors given at 1σ level)

Sample	Laboratory	Mineral	^{39}Ar (%)	Plateau age (Ma)	^{39}Ar (%)	Correlated age (Ma)	Total gas age (Ma)	Accepted age (Ma)
T0	Canada	Hornblende	82.2	187.69 \pm 0.73	95.3	185.39 \pm 0.99	189.36 \pm 0.78	185.39 \pm 0.99
T1-Arizona	Arizona	Hornblende	96.5	184 \pm 5	100	182 \pm 10	179 \pm 9	184 \pm 5
T1-Nevada	Nevada	Hornblende	44	181.6 \pm 0.7	44	182.8 \pm 2.5	180.3 \pm 0.7	182.8 \pm 1.3

exhibit zonality and polysynthetic twinning, although, in contrast to sample T0, crystals from T1 do not show resorption borders. They may sporadically have inclusions of clinopyroxene and plagioclase altered to sericite and clays. Clinopyroxene crystals are euhedral and represent 10% of the phenocryst fraction. Biotite phenocrysts are very scarce and are intensely altered to opaque minerals and chlorites. The remaining 5% of the phenocryst fraction is shared by opaque minerals and apatite. The groundmass (50% of the rock) has a microgranular appearance, and is formed by opaque minerals, plagioclase and former glass, which is devitrified to clays, chlorite and secondary silica. Veins and amygdales are filled with chlorite and silica.

Amphibole separates picked from these two samples were sent to three laboratories for $^{40}\text{Ar}/^{39}\text{Ar}$ age determinations by furnace step-heating on single grains. Sample T0 was irradiated in the nuclear reactor at McMaster University, Hamilton, Canada; sample T1-A was analysed at the Arizona Noble Gases Laboratory of the University of Arizona (USA); and sample T1-N was sent to the Nevada Isotope Geochronology Laboratory (NIGL) of the University of Nevada, Las Vegas (USA). The decay constants used were those of Steiger & Jäger (1977). Errors shown in the age spectrum and isotope correlation diagram represent the analytical precision at 1σ . The dates and J values of sample T0 are referenced to Hb3Gr hornblende at 1072 Ma (Roddick 1983), to the Fish Canyon Tuff sanidine at an age of 28.02 Ma (Renne *et al.* 1998) for sample T1-N, and to the GA 1550 Biotite flux monitors (98.79 \pm 0.54 Ma, Renne *et al.* 1998) for sample T1-A. A summary of the geochronological data is given in Table 1. Sample T0 (Fig. 2a) gave a plateau age of 187.7 \pm 0.73 Ma (1σ) for 82% of the ^{39}Ar released. Although there is no statistical difference between the plateau age and the isotope correlation age (185.4 \pm 0.99 Ma) the initial ratio is greater than atmospheric. Thus, there could be some small amount of excess argon influencing the plateau age and so the correlation age is the preferred value in our interpretation. Franzese *et al.* (2002) reported a U–Pb sensitive high-resolution ion microprobe (SHRIMP) age of 242.9 \pm 2.5 Ma for the same lava, which is incompatible with the geology because the outcrop clearly corresponds to the Jurassic Lonco Trapial Formation (i.e. the Taquetren Formation of Franzese *et al.*). Because our $^{40}\text{Ar}/^{39}\text{Ar}$ age is consistent with the regional geology, we suspect that the T0 lava carries inherited zircons from the underlying Triassic granitoids of the Central Patagonian Batholith, thus explaining the anomalous U–Pb SHRIMP age (Franzese *et al.* 2002).

Amphibole separates picked from sample T1 were divided into two aliquots (T1-N and T1-A) each sent to different laboratories as noted above. Sample T1-A (Fig. 2b) produced a good plateau age of 184 \pm 5 Ma (1σ) with almost 95% of the ^{39}Ar released. The correlated age is 182 \pm 10 Ma (1σ), and the total gas age is slightly lower (179 \pm 9 Ma, 1σ , Table 1) owing to argon loss in the less retentive sites. No excess argon seems to be present in the sample because the initial $^{40}\text{Ar}/^{36}\text{Ar}$ ratio is close to atmospheric and because the age spectrum does not show the typical U-shape of samples containing excess argon (Fig. 2c). The uncertainty in the

correlation age is somewhat high (Table 1, and see below), thus the preferred age for this sample is the plateau age.

In aliquot T1-N, Ca/K and Cl/K ratios covary (Fig. 2c) and change by >30%, which indicates that the sample contained more than one source of amphibole (see the explanations of Villa *et al.* 2000, and references therein). An isochemical age was calculated following Allaz *et al.* (2011) using the high-temperature release steps (15–17), which are the only ones with indistinguishable Ca/K ratios (25.2 \pm 0.5), indistinguishable Cl/K ratios (0.184 \pm 0.004), and also indistinguishable ages. For these steps, which together make up 44% of the ^{39}Ar release, the weighted average age is 181.6 \pm 0.7 Ma. The isochron age for these three steps is 182.8 \pm 1.3 Ma (1σ) with an initial $^{40}\text{Ar}/^{36}\text{Ar}$ ratio of 281 \pm 29 and MSWD of 0.08. The isochron age of 182.8 \pm 1.3 Ma, which is closely coincident with the plateau age, is taken as the most acceptable age for this aliquot and is consistent with the independent T1-A determination.

Palaeomagnetism

We drilled 198 samples at 24 sites irregularly covering an area of about 1800 km² in the Sierra de Lonco Trapial (Fig. 1). Sampled rock types are andesitic lavas and dykes, andesitic breccias, ignimbrites, hydrothermal breccias, fine-grained sandstones and pelites intercalated within the volcanites (Table 2). Samples were oriented using both magnetic and solar compasses. The natural remanent magnetization (NRM) of standard palaeomagnetic specimens was measured with a three-axis cryogenic magnetometer DC-SQUID (2G-750R), and the susceptibility of samples subjected to thermal demagnetization was monitored during the process using a Bartington MS-2 susceptibility meter.

The intensity of the NRM of the volcanic rocks ranged from 1 to 4000 mA m⁻¹, with the ignimbrites and andesitic lavas having the lowest and highest values, respectively. Stepwise thermal and alternating field (AF) demagnetization techniques were applied to analyse the palaeomagnetic behaviour. Six sites (mainly greenish andesites) showed only a soft, low-coercivity magnetization almost completely removed at 15–20 mT and were omitted from further study. AF demagnetization revealed that remanence in samples from sedimentary sites JZ16t and T2 is dominated by a moderate-to high-coercivity component probably carried by magnetite (e.g. Fig. 3a). In contrast, AF demagnetization removed only c. 50% of the natural magnetization in the lavas, breccias and ignimbrites (e.g. Fig. 3b), pointing to the important contribution of hematite as a remanence carrier in these rocks. Thus, thermal demagnetization was the preferred method to fully demagnetize the samples (e.g. Fig. 3c–e). A univectorial behaviour was observed in all cases, with magnetite and hematite carrying the same palaeomagnetic vector (e.g. compare results from samples of site JZ3: Fig. 3b v. Fig. 3c). From these samples carrying a high-coercivity, high-temperature magnetization, only those components having a maximum angular deviation $\leq 10^\circ$ were considered for further study.

Rock magnetism (hysteresis loops and isothermal remanent magnetization acquisition) further illustrates the almost exclusive

Table 2. Palaeomagnetic results of Lonco Trapijal Formation at Sierra de Lonco Trapijal

Site	Lat. (°S)	Long. (°W)	Lithology	J_0 (mAm ⁻¹)	n/n_0	Dec.	Inc.	α_{95}	k	VGP (°S)	VGP (°E)	dp	dm
JZ1	-42.12	-69.28	Rhyolite	1	3/5	349.2	-45.3	27.2	22	-72.3	77.3	22	35
JZ2	-42.04	-69.28	Andesite	1000	5/6	156.0	61.0	7.6	101	-72.2	12.6	8.9	12
JZ3	-41.85	-69.40	Andesite	400	5/6	165.1	29.9	3.8	574	-61.2	79.8	2.3	4.2
JZ4	-41.85	-69.30	Andesite	300	4/5	147.3	46.0	9.7	90	-59.7	38.7	7.9	12
JZ5	-41.87	-69.33	Andesite	500	6/6	171.9	59.6	5.1	172	-83.8	31.4	5.8	7.7
JZ6*	-41.88	-69.37	Andesite	1000	5/5	344.1	-37.8	5.2	312	-65.4	73.0	3.6	6.1
JZ10	-42.16	-69.12	Andesite	1000	4/5	356.0	-59.2	9.6	167	-86.3	55.3	11	14
JZ11*	-42.17	-69.13	Ignimbrite	500	5/6	142.0	37.6	6.2	153	-51.7	42.7	4.3	7.3
JZ12	-42.03	-69.11	And/ignim	300	5/8	219.6	39.9	8.4	65	-51.8	183.0	6.1	10
JZ16	-42.26	-69.41	Breccia	10	4/6	314.6	-64.5	26	13	-57.7	357.5	33	42
JZ16t	-42.26	-69.41	Tuff	10	7/9	9.6	-61.3	10.4	35	-82.9	205.0	12	16
JZ17	-42.26	-69.41	Ignimbrite	3	5/6	298.8	-52.4	16.9	21	-41.7	10.5	16	23
T2	-42.10	-69.10	Pelite	7	8/8	167.7	61.2	7.7	52	-80.9	15.6	9.1	12
T4	-42.05	-69.09	Andesite	4000	5/6	161.0	67.5	10	45	-82.2	62.2	18	19
T5	-42.14	-69.09	Rhyolite	9	9/9	2.7	-60.3	4.8	116	-87.8	177.8	5.5	7.3
T6	-42.13	-69.10	Andesite	20	6/6	14.8	-67.4	4.6	212	-77.0	244.4	6.4	7.7
T7	-42.17	-69.14	Ignimbrite	8	5/5	41.9	-46.1	5.9	170	-53.0	191.1	4.8	7.6
GTK	-42.16	-69.12	Andesite	700	4/6	350.5	-62.9	10.4	79	-82.7	0.2	13	16

J_0 , average intensity of initial natural magnetization; n/n_0 , number of collected samples/number of samples used in statistics; Dec. and Inc., declination and inclination of site mean palaeomagnetic vector; α_{95} , semiangle of the conus of 95% confidence around the mean; k , Fisherian precision parameter; VGP, virtual palaeomagnetic pole associated with each site (given in °S latitude, °E longitude); dp, semiaxis of the confidence ellipse around the VGP in the site-to-pole direction; dm, semiaxis of the ellipse in the direction normal to dp.

*After restoring to the palaeohorizontal. Bedding plane JZ6 = 270°E, dip 5°S; bedding plane JZ11 = 297°E, dip 30°NE.

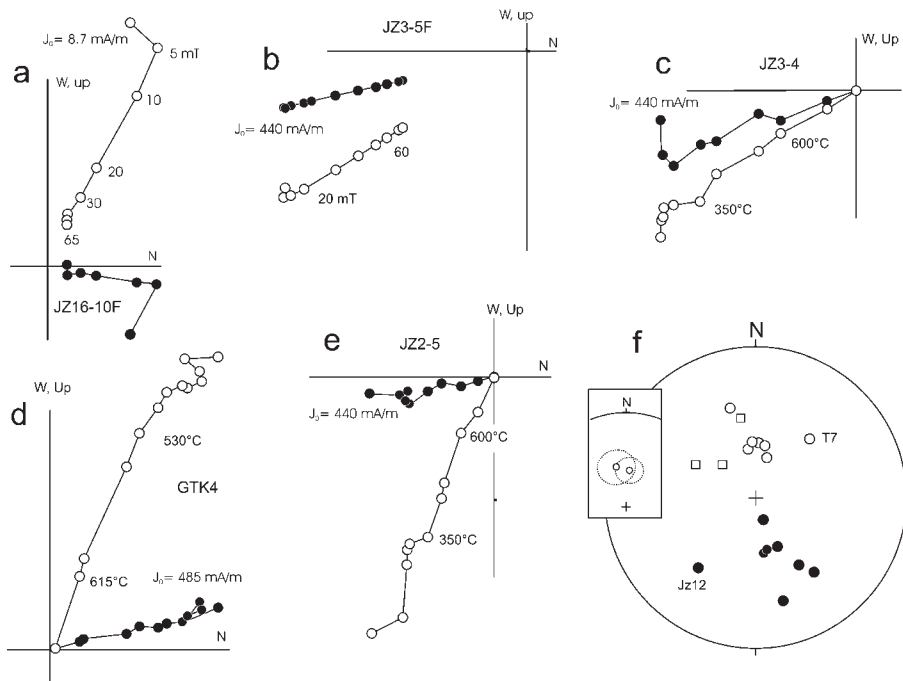


Fig. 3. (a–e) Examples of palaeomagnetic behaviour. Open (closed) symbols indicate projection onto the vertical (horizontal) plane. (f) Site mean directions with open (closed) symbols representing normal (reversed) palaeofield records. Squares denote mean direction with $\alpha_{95} > 15^\circ$. Sites JZ12 and T7 were not used for tectonic interpretation.

presence of magnetite in the sedimentary sites and the coexistence of high- and low-coercivity phases in most of the palaeomagnetically suitable volcanic rocks. Polished sections from andesites of sites GTK, JZ6 and JZ10 (e.g. Fig. 4) were examined under reflected light to further investigate the relationship between high- and low-coercivity minerals. Euhedral titanomagnetite grains in the range 100–200 μm appear disseminated in the groundmass of the andesites and are intensely oxidized to titanohematites disposed along the

{111} planes of the host titanomagnetite (Fig. 4). The oxidation textures in the titanomagnetites could be ascribed to the C4–C5 stages of Haggerty (1976). Hematite patches also appear as alteration product in amphibole phenocrysts.

The titanohematites are interpreted to be the product of high-temperature (>400 °C) deuteric processes because: (1) titanohematite in titanomagnetite is disposed along the {111} planes of the host resembling high-temperature oxidation states (C4 and C5 of

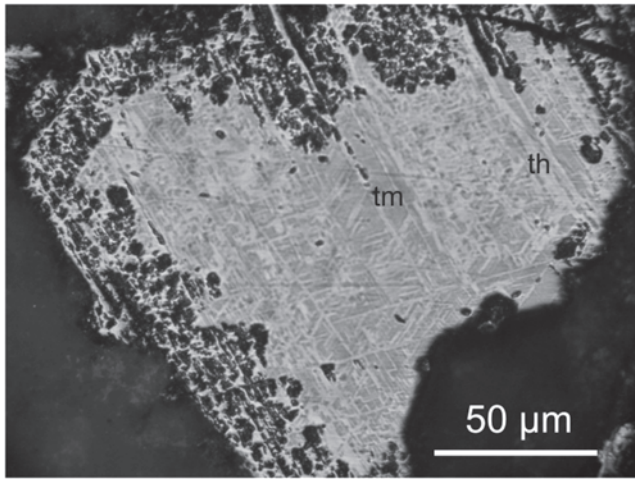


Fig. 4. Photomicrograph of highly oxidized titanomagnetite grain in sample GTK6. Titanohematite is disposed along {111} planes of the host resembling stages C4 and C5 of Haggerty (1976). Higher oxidation in the border of the grain led to complete replacement of titanomagnetite by rutile. Parallel Nicols. th, titanohematite; tm, titanomagnetite.

Haggerty 1976); (2) titanomagnetite and titanohematite carry the same palaeomagnetic component (compare Fig. 3b with Fig. 3c), pointing to almost simultaneous blocking of their remanences; (3) site mean palaeomagnetic vectors define a population of normal and reversed directions whose dispersion (Fig. 3f) resembles that expected for natural (palaeosecular) variation of the palaeomagnetic field instead of the tight clustering of directions typically seen in the cases of regional remagnetization; (4) regional remagnetization should also have affected the sedimentary sites JZ16t and T2, which show opposite polarities and magnetite as the principal carrier; (5) the Lonco Trapial volcanic rocks represent the last thermal event in the sampling area, with the exception of a small, isolated Quaternary basalt cropping out in a gorge carved in the Gastre granitoids of the Sierra de Lonco Trapial. We conclude that the observed remanences in the lavas constitute records of the Early Jurassic geomagnetic field, in part of thermoremanent nature (titanomagnetites) and partly reflecting high-temperature, deuteric oxidation processes (thermoremanent and/or thermochemical) that occurred during and immediately after the emplacement of the lavas, ignimbrites and volcanic breccias. The remanence from the two sedimentary sites, showing opposite polarities and magnetite as the almost unique carrier, was therefore probably acquired at or soon after deposition.

A mean direction for each site was obtained by applying standard Fisherian statistics (Table 2). At site level we choose an $\alpha_{95} \leq 15^\circ$ cutoff angle for admission of results, resulting in the rejection of the mean direction from three of the sites listed in Table 2. Normal and reversed site mean directions are separated by $11^\circ \pm 14^\circ$ arc (see inset in Fig. 3f) yielding a positive class C reversal test (McFadden & McElhinny 1990), which strongly suggests that the time-averaged palaeomagnetic vector constitutes an acceptable determination of the palaeofield and is valid for further tectonic interpretations. Site mean magnetizations from the 15 sites that passed the selection criteria were converted to virtual geomagnetic poles (VGP, Table 2) to compute a mean pole position. VGPs from two of these sites (JZ12 and T7; their vectors are denoted in Fig. 3f) were discarded because they are removed by more than 2σ from the mean pole position of the first ($n=15$) run. Finally, a mean pole position for the 13 accepted sites of the Lonco Trapial Formation at Gastre was determined (79.35°S , 47.01°E , $A_{95} = 8.4^\circ$, $K = 26$).

Early Jurassic tectonomagmatic overview of the North Patagonian Massif

The new ^{40}Ar – ^{39}Ar ages from the Lonco Trapial unit allow an almost complete view of Early Jurassic palaeogeography across the North Patagonian Massif (Fig. 5). From west to east, the main tectonic units representing this palaeogeography are: (1) a forearc mostly composed of marginal sedimentary prisms accreted to the continental margin in the Late Palaeozoic (north of $c. 41^\circ 30'\text{S}$) and latest Triassic–earliest Jurassic times (Duhart *et al.* 2001; Hervé & Fanning 2001; Hervé *et al.* 2003); (2) the Subcordilleran Plutonic Belt, representing an unroofed 180–185 Ma magmatic arc (Rapela *et al.* 2005); (3) the strata of the NNW–SSE-trending Pampa de Agnia Basin, which contain late Pliensbachian–Toarcian ammonites (Lesta *et al.* 1980; Uliana & Biddle 1987; Vizán 1998); (4) the herein dated Lonco Trapial volcano-sedimentary suite (Page & Page 1993); (5) the Marifil rhyolite–ignimbrite field (Pankhurst & Rapela 1995; Féraud *et al.* 1999) cropping out from central Patagonia eastward to the Atlantic coast (Fig. 5).

The $c. 185$ Ma Lonco Trapial andesites in Gastre overlie $c. 210$ Ma granitoids of the Central Patagonian Batholith, constraining uplift and denudation of the batholith to a $c. 25$ Ma interval coinciding with the Triassic–Jurassic boundary. This interval includes the Chonide event, which represents the metamorphism and final accretion of the southern Andean Chonos and Madre de Dios accretionary complexes (Thomson & Hervé 2002; Hervé *et al.* 2003, 2008). The Chonide event, in turn, seems to be coeval with the Peninsula Orogeny in West Antarctica and with the Rangitata I Orogeny in New Zealand (e.g. Vaughan & Livermore 2005), suggesting that uplift and denudation of the Central Patagonian batholith in Gastre may have been associated with an accretionary episode of regional extent along the proto-Pacific margin of Gondwana.

The new $^{40}\text{Ar}/^{39}\text{Ar}$ ages further indicate that the Lonco Trapial calc-alkaline lavas (LT in Fig. 5) were erupted in the eastern side of the evolving Pampa de Agnia Basin. Farther east, Early Jurassic magmatic activity produced the extensive Marifil rhyolite–ignimbrite field (MF in Fig. 5). Similar isotopic ages found for both the Lonco Trapial and the Marifil units (Féraud *et al.* 1999; Pankhurst *et al.* 2000; this paper) agree with the observed interdigitation between the (eastern) rhyolites and the (western) andesites near 67°W (Lesta *et al.* 1980). The composition of the western lavas was interpreted as the result of fractional crystallization of mantle-derived material with a subduction geochemical signature (Page & Page 1993). The eastern rhyolitic province is thought to be the result of extensive anatexis of the lower crust, producing initially primary andesitic magmas that later underwent crystal–liquid fractionation processes involving fractional crystallization and remelting during magma ascent (Pankhurst & Rapela 1995). Thus, extensional tectonics would have been the likely mechanism to produce melting in the eastern silicic sector. Although the western mafic volcanic rocks have a subduction-related signature indicating their active-margin association along with the Early Jurassic granitoids of the Subcordilleran Plutonic Belt, the participation of extension in magma generation here is also likely (e.g. Gust *et al.* 1985; Uliana *et al.* 1985), as indicated by coeval development of the adjacent, fault-bounded Pampa de Agnia Basin.

Analysing the Pliensbachian–Toarcian palaeomagnetic record in northern Patagonia

The tectonic analysis of deformed regions and suspect terranes requires the comparison between observed and expected

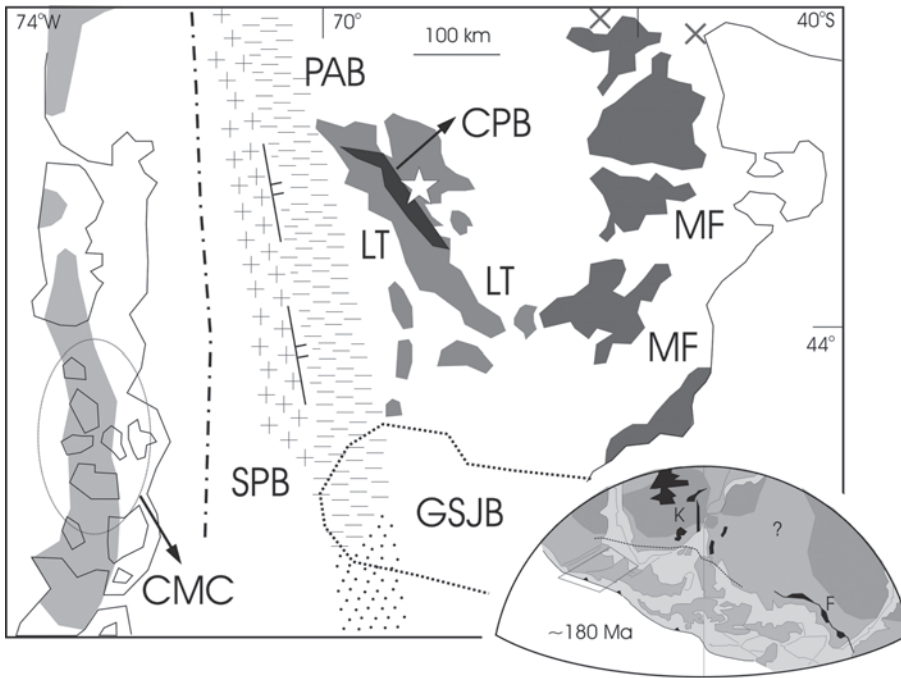


Fig. 5. Main *c.* 185 Ma tectonic units in the North Patagonian Massif, from west to east: the Chonos accretionary complex (CMC), the Subcordilleran Plutonic Belt (SPB), the Pampa de Agnia Basin (PAB), the Lonco Trapial volcanic field (LT) and the Marifil volcanic field (MF), both of the last two covering an area greater than 200000 km². Crosses in the upper right corner denote outcrops of *c.* 180 Ma plutons. CPB, Late Triassic Central Patagonian Batholith; dashed-dotted line, axis of the Middle Jurassic to Neogene Patagonian Batholith; GSJB, Mid- to Late Jurassic to Cretaceous Golfo de San Jorge Basin. Inset shows the region in a *c.* 180 Ma palaeogeography of Gondwana after Dalziel *et al.* (2000), with the old cratonic nuclei shaded dark grey and the Karoo–Ferrar (K and F, respectively) LIP shaded black.

palaeomagnetic directions for the studied locality, the expected directions being derived from the coeval palaeomagnetic field in stable areas (the reference palaeofield). A common approach for performing this is to compare the obtained data with reference poles from global compilations (e.g. Besse & Courtillot 2002; Torsvik *et al.* 2008), which fill gaps in the available data for single plates and average out unknown residual problems with the selected poles (e.g. Somoza 2011). In the case of our study, however, we may compare the results with two indisputable Early Jurassic cratonic poles for Gondwana, namely the palaeopoles from the *c.* 180 Ma lavas and intrusive rocks of the Karoo (averaging six poles listed by Torsvik *et al.* 2008) and Ferrar (as determined by Lanza & Zanella 1993) large igneous provinces cropping out in the Kalahari and East Antarctica cratons, respectively.

The three available poles from 178–186 Ma rocks in the North Patagonian Massif together with the above reference poles for cratonic Gondwana in South American coordinates, and an additional cratonic pole from coeval dykes and lavas in NE Brazil (Ernesto *et al.* 2003), are shown in Figure 6. The North Patagonian poles arise from studies in (1) dominantly sedimentary rocks from the Lepa and Osta Arena Formations in the Pampa de Agnia Basin (Vizán 1998; LO in Fig. 6), (2) rhyolitic lavas and ignimbrites from the Marifil Formation at Peninsula Camarones (Iglesia Llanos *et al.* 2003; MF in Fig. 6), and (3) the palaeopole of this study from the Lonco Trapial Formation (LT in Fig. 6). All three North Patagonian poles are offset from the reference poles, with the main contrast being in the mean declination of their time-averaged palaeomagnetic vectors. The palaeolatitudes predicted by the Early Jurassic volcanic rocks (MF and LT in Fig. 6) are in close agreement with each other and as predicted by the reference poles, whereas the lower palaeolatitude predicted by the pole from the Lepa and Osta Arena formations (LO in Fig. 6) could be related to inclination flattening associated with compaction processes in the Pampa de Agnia basin. The overall picture suggests that these localities in the North Patagonian Massif record variable amounts of anticlockwise finite rotation with respect to cratonic South America, with very low to negligible latitudinal motion.

The internal difference between the Patagonian poles in Figure 6 may result from either coeval differential rotation in small crustal blocks and/or the accumulation of rotations from differing subsequent events at one or more localities. The latter must be taken into account given the presence of pre-mid-Cretaceous clockwise (opposite sense) rotations detected in rocks of the Middle to Upper Jurassic Cañadón Asfalto Formation cropping out *c.* 200 km south of Gastre (Geuna *et al.* 2000) and possibly also in 170 Ma dykes located *c.* 70 km WNW of Gastre (Rapalini & López de Luchi 2000), although the latter could alternatively be a case of unresolved eastward tilting. Overall, the data in Figure 6 together with those in previous studies (Geuna *et al.* 2000; Somoza *et al.* 2008) indicate that the pre-mid-Cretaceous palaeomagnetic record in Patagonia should not be incorporated in the cratonic palaeopole database for South America but should be analysed in terms of internal Patagonian deformation. Indeed, it is likely that, during the early breakup of Gondwana, the Patagonia–West Antarctica region behaved as a collection of single blocks moving towards the ancestral Pacific in the frame of widespread extensional tectonics (e.g. Barker 1999). In this context, the increasing palaeomagnetic database from southern South American localities of this former collection of West Gondwana Pacific borderland blocks shows a kinematic complexity resembling that already observed from those blocks that form the present-day West Antarctica and New Zealand landmasses (see discussion by DiVenere *et al.* 1996).

The kinematics indicated by palaeomagnetic data from Lower Jurassic rocks in the North Patagonian Massif, which incorporates results from two localities along the supposed tectonic junction of the Gastre Fault System (LT and CP in Fig. 6, see also Fig. 1), strongly contrasts with the large clockwise rotation detected in the roughly coeval (e.g. Stone *et al.* 2008) dolerites of the Falkland/Malvinas Islands (Taylor & Shaw 1989). This argues against a direct kinematic relationship between the rotation of the islands and the deformation in the Gastre area (e.g. Rapela & Pankhurst 1992; Marshall 1994; Martin 2007), further supporting the findings in new studies (von Gosen & Loske 2004; Zaffarana *et al.* 2010,

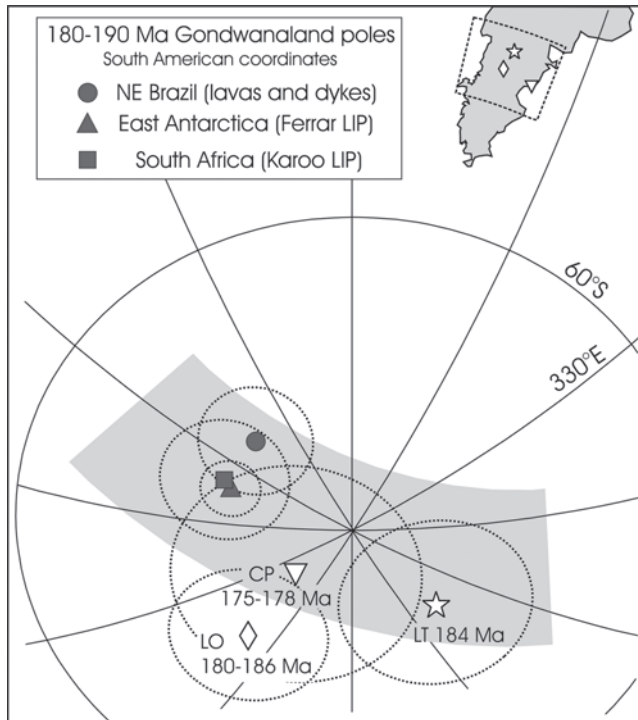


Fig. 6. The *c.* 185–180 Ma palaeomagnetic poles for the North Patagonian Massif. CP, Marifil Formation from Peninsula Camarones; LO, Lepa–Ostarena formations from the Pampa de Agnia Basin; LT, palaeopole from the Sierra de Lonco Trapial. Reference poles correspond to the *c.* 180 Ma poles from the Karoo (average of six poles listed by Torsvik *et al.* 2008) and Ferrar (Lanza & Zanella 1993) large igneous provinces plus a pole from lavas and intrusive rocks in NE Brazil (Ernesto *et al.* 2003). Shaded zone shows a palaeocolatitudinal sector enclosing most of the poles of the figure. The sampling localities of each of the North Patagonian poles are shown.

2012) that oppose the existence of the Gastre Fault System as a regional, through-going dextral fault system of transcontinental dimensions during the breakup of Gondwana.

Conclusions

The new *c.* 185 Ma $^{40}\text{Ar}/^{39}\text{Ar}$ age for andesites of the Lonco Trapial Formation at Gastre indicate a volcanic-dominated, Pliensbachian–Toarcian palaeogeography across the whole of the North Patagonian Massif. The rocks of the Lonco Trapial Formation lie on 210–220 Ma granitoids of the Central Patagonian Batholith, implying a period of batholith uplift and denudation in latest Triassic to earliest Jurassic times. The uplift of the Central Patagonian Batholith could thus be related to the association of events in the proto-Andean continental margin that Hervé *et al.* (2003) grouped into the Chonide Orogeny.

The palaeomagnetic poles from three Early Jurassic localities in the North Patagonian Massif show the existence of anticlockwise finite rotations of rather small and variable magnitude. These data strongly contrast with the palaeomagnetic results from the roughly coeval (Stone *et al.* 2008) dolerites in the Falkland/Malvinas Islands, arguing against a kinematic relationship between the rotation in the islands and the deformation in Gastre. Taken together, available palaeomagnetic data from Patagonia suggest a more complex than previously thought pattern of deformation during the

early stages of Gondwana breakup. The terrane boundaries in the region remain to be determined.

We thank D. Alvarez and N. Auciello for help in the field. S. Singer and S. Crosta helped with the interpretation of polished sections. C. W. Rapela provided useful comments on an early version of the paper. Helpful reviews by R. Lanza and G. Taylor greatly improved the final version. Special thanks go to I. Villa (Associate Editor) for his valuable help with the treatment and presentation of geochronological data. The field trip was supported by ANPCyT PICT 1074-2006. Isotopic dates were supported by CONICET PIP 112-200801-02828.

References

- ADIE, R.J. 1952. The position of the Falkland Islands in a reconstruction of Gondwanaland. *Geological Magazine*, **89**, 401–410.
- ALLAZ, J., EUGI, M., BERGER, A. & VILLA, I.M. 2011. The effects of retrograde reactions and of diffusion on $^{40}\text{Ar}/^{39}\text{Ar}$ ages of micas. *Journal of Petrology*, **52**, 691–716.
- BARKER, P.F. 1999. Falkland Plateau evolution and a mobile southernmost South America. In: CAMERON, N.R., BATE, R.H. & CLURE, V.S. (eds) *The Oil and Gas Habitats of the South Atlantic*. Geological Society, London, Special Publications, **153**, 403–408.
- BEN-AVRAHAM, Z., HARTNADY, C.J.H. & MALAN, J.A. 1993. Early tectonic extension between the Agulhas Bank and the Falkland Plateau due to rotation of the Lafonia Microplate. *Earth and Planetary Science Letters*, **117**, 43–58.
- BESSE, J. & COURTILOT, V. 2002. Apparent and true polar wander and the geometry of the geomagnetic field over the last 200 Myr. *Journal of Geophysical Research*, **107**, 2300, doi:10.1029/2000JB000050.
- CURTIS, M.L. & HYAM, D.M. 1998. Late Palaeozoic to Mesozoic structural evolution of the Falkland Islands: a displaced segment of the Cape Fold Belt. *Journal of the Geological Society, London*, **155**, 115–129.
- DALZIEL, I.W. & GRUNOW, A.M. 1992. Late Gondwanide tectonic rotations within Gondwanaland. *Tectonics*, **11**, 603–606.
- DALZIEL, I.W.D., LAWVER, L.A. & MURPHY, J.B. 2000. Plumes, orogenesis, and supercontinental fragmentation. *Earth and Planetary Science Letters*, **178**, 1–11.
- DI VENERE, V., KENT, D.V. & DALZIEL, I.W.D. 1996. Summary of palaeomagnetic results from West Antarctica: implications for the tectonic evolution of the Pacific margin of Gondwana during the Mesozoic. In: STOREY, B.C., KING, E.C. & LIVERMORE, R.A. (eds) *Weddell Sea Tectonics and Gondwana Break-Up*. Geological Society, London, Special Publications, **108**, 31–43.
- DUHART, P., McDONOUGH, M., MUÑOZ, J., MARTIN, M. & VILLENEUVE, M. 2001. El Complejo Metamórfico Bahía Mansa en la Cordillera de la Costa del centro-sur de Chile (39°30′–42°00′S): geocronología K–Ar, $^{40}\text{Ar}/^{39}\text{Ar}$ y U–Pb e implicancias en la evolución del margen sur-occidental de Gondwana. *Revista Geológica de Chile*, **28**, 179–208.
- EAGLES, G. & VAUGHAN, A.P.M. 2009. Gondwana breakup and plate kinematics: business as usual. *Geophysical Research Letters*, **36**, L10302, doi:10.1029/2009GL037552.
- ERNESTO, M., BELLINI, G., *ET AL.* 2003. Paleomagnetic and geochemical constraints on the timing and duration of the CAMP activity in northeastern Brazil. In: HAMES, W., MCHONE, J.G., RENNE, P. & RUPPEL, C. (eds) *The Central Atlantic Magmatic Province: Insights from Fragments of Pangea*. American Geophysical Union, Geophysical Monograph, **136**, 129–149.
- FÉRAUD, G., ALRIC, V., FORNARI, M., BERTRAND, H. & HALLER, M. 1999. $^{40}\text{Ar}/^{39}\text{Ar}$ dating of the Jurassic volcanic province of Patagonia: migrating magmatism related to Gondwana break-up and subduction. *Earth and Planetary Science Letters*, **172**, 83–96.
- FRANZESE, J.R., PANKHURST, R.J., RAPELA, C.W., SPALLETI, L.A., FANNING, C.M. & MURAVCHICK, M. 2002. Nuevas evidencias geocronológicas sobre el magmatismo gondwánico en el noroeste del Macizo Norpatagónico. In: CINGOLANI, C.A., CABALIERI, N., LINARES, E., LÓPEZ DE LUCHI, M.G., OSTERA, H.A. & PANARELLO, H.O. (eds) *XV Congreso Geológico Argentino*. Asociación Geológica Argentina, Buenos Aires, **1**, 144–148.
- GEUNA, S., SOMOZA, R., VIZÁN, H., FIGARI, E. & RINALDI, C. 2000. Paleomagnetism of Jurassic and Cretaceous rocks in central Patagonia: a key to constrain the timing of rotations during the breakup of southwestern Gondwana? *Earth and Planetary Science Letters*, **181**, 145–160.
- GUST, D.A., BIDDLE, K.T., PHELPS, D.W. & ULIANA, M.A. 1985. Associated Middle to Late Jurassic volcanism and extension in southern South America. *Tectonophysics*, **116**, 223–253.
- HAGGERTY, S.E. 1976. Oxidation of opaque mineral oxides in basalts. In: Rumble, D. (ed.) *Oxide Minerals*. Mineralogical Society of America, Short Course Notes, **3**, Hg1–Hg100.

- HERVÉ, F. & FANNING, C.M. 2001. Late Triassic zircons in metaturbidites of the Chonos Metamorphic Complex, southern Chile. *Revista Geológica de Chile*, **28**, 91–104.
- HERVÉ, F., FANNING, C.M. & PANKHURST, R.J. 2003. Detrital zircon age patterns and provenance of the metamorphic complexes of southern Chile. *Journal of South American Earth Sciences*, **16**, 107–123.
- HERVÉ, F., CALDERÓN, M. & FAÚNDEZ, V. 2008. The metamorphic complexes of the Patagonian and Fuegian Andes. *Geologica Acta*, **6**, 43–53.
- IGLESIA LLANOS, M.P., LANZA, R., RICCARDI, A.C., GEUNA, S.E., LAURENZI, M.A. & RUFFINI, R.R. 2003. Palaeomagnetic study of the El Quemado complex and Marifil formation, Patagonian Jurassic igneous province, Argentina. *Geophysical Journal International*, **154**, 599–617.
- KÖNIG, M. & JOKAT, W. 2006. The Mesozoic breakup of the Weddell Sea. *Journal of Geophysical Research*, **111**, B12102, doi:10.1029/2005JB004035.
- LANZA, R. & ZANELLA, E. 1993. Palaeomagnetism of the Ferrar dolerite in the northern Prince Albert Mountains (Victoria Land, Antarctica). *Geophysical Journal International*, **114**, 501–511.
- LESTA, P., FERELLO, R. & CHEBLI, G. 1980. Chubut extraandino. In: TURNER, J.C.M. (ed.) *Segundo Simposio de Geología Regional Argentina*. Academia Nacional de Ciencias, Córdoba, **2**, 1307–1380.
- MARSHALL, J.E.A. 1994. The Falkland Islands: a key in Gondwana geography. *Tectonics*, **13**, 499–514.
- MARTIN, A.K. 2007. Gondwana breakup via double-saloon-door rifting and seafloor spreading in a backarc basin during subduction rollback. *Tectonophysics*, **445**, 245–272.
- McFADDEN, P.L. & McELHINNY, M.W. 1990. Classification of the reversal test in magnetism. *Geophysical Journal International*, **103**, 725–729.
- PAGE, R. & PAGE, S. 1993. Petrología y significado tectónico del Jurásico volcánico del Chubut central. *Revista de la Asociación Geológica Argentina*, **48**, 41–58.
- PANKHURST, R.J. & RAPELA, C.W. 1995. Production of Jurassic rhyolite by anatexis in the lower crust of Patagonia. *Earth and Planetary Science Letters*, **134**, 23–36.
- PANKHURST, R.J., RILEY, T.R., FANNING, C.M. & KELLEY, S.P. 2000. Episodic silicic volcanism in Patagonia and the Antarctic Peninsula: chronology of magmatism associated with the break-up of Gondwana. *Journal of Petrology*, **41**, 605–625.
- RAPALINI, A. & LÓPEZ DE LUCHI, M.G. 2000. Palaeomagnetism and magnetic fabric of Middle Jurassic dykes from western Patagonia, Argentina. *Physics of the Earth and Planetary Interiors*, **120**, 11–27.
- RAPELA, C.W. & PANKHURST, R.J. 1992. The granites of northern Patagonia and the Gastre Fault System in relation to the break-up of Gondwana. In: STOREY, B.C., ALABASTER, T. & PANKHURST, R.J. (eds) *Magmatism and the Causes of Continental Break-Up*. Geological Society, London, Special Publications, **68**, 209–220.
- RAPELA, C.W., PANKHURST, R.J. & HARRISON, S.M. 1992. Triassic ‘Gondwana’ granites of the Gastre district, North Patagonian Massif. *Transactions of the Royal Society of Edinburgh, Earth Sciences*, **83**, 291–304.
- RAPELA, C.W., PANKHURST, R.J., FANNING, C.M. & HERVÉ, F. 2005. Pacific subduction coeval with the Karoo mantle plume: the Early Jurassic subcordilleran belt of northwestern Patagonia. In: VAUGHAN, A.P.M., LEAT, P.T. & PANKHURST, R.J. (eds) *Terrane Processes and the Margins of Gondwana*. Geological Society, London, Special Publications, **246**, 217–239.
- RENNE, P.R., SWISHER, C.C., DEINO, A.L., KARNER, D.B., OWENS, T.L. & DEPAOLO, D.J. 1998. Intercalibration of standards, absolute ages and uncertainties in $^{40}\text{Ar}/^{39}\text{Ar}$ dating. *Chemical Geology*, **145**, 117–152.
- RODDICK, J.C. 1983. High precision intercalibration of $^{40}\text{Ar}/^{39}\text{Ar}$ standards. *Geochimica et Cosmochimica Acta*, **47**, 887–898.
- SILVA NIETO, D.G. 2005. *Hoja Geológica 4369-III, Paso de Indios. Escala 1:250.000*. Instituto de Geología y Recursos Minerales. Servicio Geológico Minero Argentino, Boletín, 267.
- SOMOZA, 2011. The Late Cretaceous paleomagnetic field in North America: a South American perspective. *Canadian Journal of Earth Sciences*, **48**, 1483–1488.
- SOMOZA, R., VIZÁN, H. & TAYLOR, G.K. 2008. Tectonic rotations in the Deseado Massif (Patagonia) during the break-up of Gondwana. *Tectonophysics*, **460**, 178–185.
- STEIGER, R.H. & JÄGER, E. 1977. Subcommittee on geochronology: convention on the use of decay constants in geo- and cosmo-chronology. *Earth and Planetary Science Letters*, **36**, 359–362.
- STONE, P., RICHARDS, P.C., KIMBELL, G.S., ESSER, R.P. & REEVES, D. 2008. Cretaceous dykes discovered in the Falkland Islands: implications for regional tectonics in the South Atlantic. *Journal of the Geological Society, London*, **165**, 1–4.
- TAYLOR, G.K. & SHAW, J. 1989. The Falkland Islands: new palaeomagnetic data and their origin as a displaced terrane from southern Africa. In: WILLHOUSE, J.W. (ed.) *Deep Structure and Past Kinematics of Accreted Terranes*. American Geophysical Union, Geophysical Monographs, **50**, 59–72.
- THOMSON, S.N. & HERVÉ, F. 2002. New time constraints for the age of metamorphism at the ancestral Pacific Gondwana margin of southern Chile (42–52°S). *Revista Geológica de Chile*, **29**, 151–165.
- TORSVIK, T.H., MÜLLER, R.D., VAN DER VOO, R., STEINBERGER, B. & GAINA, C. 2008. Global plate motion frames: toward a unified model. *Reviews of Geophysics*, **46**, 1–44.
- ULIANA, M.A. & BIDDLE, K.T. 1987. Permian to Late Cenozoic evolution of northern Patagonia: main tectonic events, magmatic activity, and depositional trends. In: MCKENZIE, G.D. (ed.) *Gondwana Six: Structure, Tectonics and Geophysics*. American Geophysical Union, Geophysical Monographs, **40**, 271–286.
- ULIANA, M.A., BIDDLE, K.T., PHELPS, D. & GUST, D. 1985. Significado del volcanismo y extensión mesojurásicos en el extremo meridional de sudamérica. *Revista de la Asociación Geológica Argentina*, **40**, 231–253.
- VAUGHAN, A.P.M. & LIVERMORE, R.A. 2005. Episodicity of Mesozoic terrane accretion along the Pacific margin of Gondwana: implications for superplume–plate interactions. In: VAUGHAN, A.P.M., LEAT, P.T. & PANKHURST, R.J. (eds) *Terrane Processes and the Margins of Gondwana*. Geological Society, London, Special Publications, **246**, 143–178.
- VILLA, I.M., HERMANN, J., MÜNTENER, O. & TROMMSDORFF, V. 2000. $^{39}\text{Ar}/^{40}\text{Ar}$ dating of multiply zoned amphibole generations (Malenco, Italian Alps). *Contributions to Mineralogy and Petrology*, **140**, 363–381.
- VIZÁN, H. 1998. Paleomagnetism of the Lower Jurassic Lepá and Osta Arena formations, Argentine Patagonia. *Journal of South American Earth Sciences*, **11**, 333–350.
- VON GOSEN, W. & LOSKE, W. 2004. Tectonic history of Calcatapul Formation, Chubut Province, Argentina, and the ‘Gastre Fault System’. *Journal of South American Earth Sciences*, **18**, 73–88.
- ZAFFARANA, C.B., LÓPEZ DE LUCHI, M.G., SOMOZA, R., MERCADER, R., GIACOSA, R. & MARTINO, R.D. 2010. Anisotropy of magnetic susceptibility study in two classical localities of the Gastre Fault System, central Patagonia. *Journal of South American Earth Sciences*, **30**, 151–166.
- ZAFFARANA, C. B., MONTENEGRO, T. & SOMOZA, R. 2012. The host rock of the Central Patagonian Batholith in Gastre: further insights on the Late Triassic to Early Jurassic deformation in the region. *Revista de la Asociación Geológica Argentina*, **69**, in press.



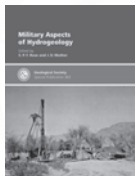
The
Geological
Society

servicing science & profession

From the Geological Society Publishing House

For full details see the Online Bookshop: www.geolsoc.org.uk/bookshop

NEW



• ISBN: 978-1-86239-340-0
• January 2011

• 376 pages • Hardback

• Prices: List: **£110.00/US\$220.00**
GSL: **£55.00/US\$110.00**

Other qualifying societies:
£66.00/US\$132.00 (Cat no tbc)
Online bookshop code: SP362

• **Special Publication 362**

Military Aspects of Hydrogeology

Edited by E. P. F. Rose and J. D. Mather

This book, generated under the auspices of the Geological Society of London's History of Geology and Hydrogeological Groups, contains 20 papers from authors in the UK, USA, Germany and Austria. Historically, it gives examples of the influence of groundwater on battlefield tactics and fortress construction; describes how groundwater was developed for water supply and overcome as an obstacle to military engineering and cross-country vehicular movement by both sides in World Wars I and II; and culminates with examples of the application of hydrogeology to site boreholes in recent conflicts, notably in Afghanistan. Examples of current research described include hydrological model development; the impact of variations in soil moisture on explosive threat detection and cross-country vehicle mobility; contamination arising from defence sites and its remediation; privatization of water supplies; and the equitable allocation of resources derived from an international transboundary aquifer.

NEW



• ISBN: 978-1-86239-339-4
• January 2011

• 232 pages • Hardback

• Prices:
List: **£80.00/US\$160.00**
GSL: **£40.00/US\$80.00**

Other qualifying societies:
£48.00/US\$96.00 (Cat no tbc)
Online bookshop code: SP361

• **Special Publication 361**

**Natural Hazards in the Asia-Pacific Region:
Recent Advances and Emerging Concepts**

Edited by J. P. Terry and J. Goff

Even a cursory glance at any map of the Asia-Pacific region makes a striking impression: in addition to the large continental landmass the region encompasses a truly vast expanse of ocean, dispersed over which are thousands of islands. Many might say that it could not be a worse time to live in this region. In the past few years we have experienced not only a number of devastating tsunamis (Indonesia, Solomon Islands, Samoa, Japan), but should not forget either the seemingly endless list of other natural hazards such as tropical cyclones and typhoons, volcanic eruptions, river floods and wildfires, amongst numerous others. This Special Publication represents an important collection of both conceptual and first-hand field investigations across the Asia-Pacific region. By highlighting some of the recent advances and emerging ideas in natural hazards research, the volume draws together these disparate lines of evidence into a clear regional focus.

NEW



• ISBN: 978-1-86239-330-1
• August 2011

• 320 pages • Hardback

• Prices:
List: **£100.00/US\$200.00**
GSL: **£50.00/US\$100.00**

Other qualifying societies:
£60.00/US\$120.00 (Cat no tbc)
Online bookshop code: SP356

• **Special Publication 356**

Martian Geomorphology

Edited by M. R. Balme, G. Sanjeev, C. Gallagher and A. Bargery

The latest Mars missions are returning data of unprecedented fidelity in their representation of the martian surface. New data include images with spatial resolution better than 30 cm per pixel, stereo imaging-derived terrain models with one meter postings, high-resolution imaging spectroscopy, and RADAR data that reveal subsurface structure. This book reveals how this information is being used to understand the evolution of martian landscapes, and includes topics such as fluvial flooding, permafrost and periglacial landforms, debris flows, deposition and erosion of sedimentary material, and the origin of lineaments on Phobos, the larger martian moon. Contemporary remote sensing data of Mars, on a par with those of Earth, reveal landscapes strikingly similar to regions of our own planet, so this book will be of interest to Earth scientists and planetary scientists alike. An overview chapter summarising Mars' climate, geology and exploration is included for the benefit of those new to Mars.

NEW



• ISBN: 978-1-86239-325-7
• February 2011

• 208 pages • Hardback

• Prices:
List: **£90.00/US\$180.00**
GSL: **£45.00/US\$90.00**

Other qualifying societies:
£54.00/US\$108.00 (Cat no 1130)
Online bookshop code: SP352

• **Special Publication 352**

**Human Interactions with the Geosphere:
The Geoarchaeological Perspective**

Edited by L. Wilson

Human impact on our environment is not a new phenomenon. For millennia, humans have been coping with – or provoking – environmental change. We have exploited, extracted, over-used, but also in many cases nurtured, the resources that the geosphere offers. Geoarchaeology studies the traces of human interactions with the geosphere and provides the key to recognizing landscape and environmental change, human impacts and the effects of environmental change on human societies.

This collection of papers from around the world includes case studies and broader reviews covering the time period since before modern human beings came into existence up until the present day. To understand ourselves, we need to understand that our world is constantly changing, and that change is dynamic and complex. Geoarchaeology provides an inclusive and long-term view of human–geosphere interactions and serves as a valuable aid to those who try to determine sustainable policies for the future.

Order from:
www.geolsoc.org.uk/bookshop

Lyell
Collection

The Geological Society's Lyell Collection: journals, Special Publications and books online. For more information visit www.geolsoc.org.uk/LyellCollection